

# Sintering and electrical properties of $\text{Bi}_4\text{Ti}_{2.95}\text{W}_x\text{O}_{11.9+3x}$ piezoelectric ceramics

M. Villegas\*, T. Jardiel, G. Farías

*Department of Electroceramics. Instituto de Cerámica y Vidrio, CSIC—Campus Universidad Autónoma de Madrid, 28049 Cantoblanco, Madrid, Spain*

## Abstract

Bismuth titanate (BIT) based ceramics doped with different amounts of  $\text{WO}_3$  were prepared by a chemical route. BIT compound was obtained by hydroxide coprecipitation method and subsequent treatment at 650 °C. The addition of the dopant was performed after calcination by surface doping using an organometallic W-compound in solution. Different amounts of dopant produce different densification behaviour because of changes in the vacancies concentration and secondary phases. Consequently, the microstructure, as well as the electrical properties, are strongly dependent on the dopant concentration. The presence of a minor amount of secondary phase in the W-doped BIT drastically decreases dielectric losses up to high temperatures allowing the polarization of the ceramics and, in consequence, a relatively good piezoelectric response with  $d_{33}$  constants up to 20.

© 2003 Elsevier Ltd. All rights reserved.

*Keywords:* Dielectric properties; Electrical conductivity; Grain size; Piezoelectric properties; Powders-chemical preparation

## 1. Introduction

Bismuth titanate ( $\text{Bi}_4\text{Ti}_3\text{O}_{12}$ ) belongs to the Aurivillius compounds family<sup>1</sup> that can be represented by the general formula  $(\text{Bi}_2\text{O}_2)^{2-}(\text{A}_{m-1}\text{B}_m\text{O}_{3m+1})^{2+}$  in which A can be a monovalent ( $\text{Na}^+$ ,  $\text{K}^+$ ), divalent ( $\text{Pb}^{2+}$ ,  $\text{Ba}^{2+}$ ) or trivalent ( $\text{Bi}^{3+}$ ,  $\text{La}^{3+}$ ) cation or a mixture of them, B represents  $\text{Ti}^{4+}$ ,  $\text{Nb}^{5+}$ ,  $\text{Ta}^{5+}$ ..., and  $m$  can have values of 2, 3, 4... In  $\text{Bi}_4\text{Ti}_3\text{O}_{12}$   $m=3$  and the crystal structure can be described as formed by three unit cells of  $\text{BiTiO}_3$  with perovskite-like structure interleaved with  $(\text{Bi}_2\text{O}_2)^{2+}$  layers. At room temperature  $\text{Bi}_4\text{Ti}_3\text{O}_{12}$  is monoclinic ( $C_{1h}=m$ ) and ferroelectric, but can be represented as orthorhombic with the  $c$ -axis normal to the  $(\text{Bi}_2\text{O}_2)^{2+}$  layers.<sup>2</sup> The ferroelectric to paraelectric phase transition in pure BIT is 675 °C and the high temperature symmetry is tetragonal ( $D_{4h}=4$  mm). The main component of the spontaneous polarization ( $P_s \approx 50 \mu\text{C}/\text{cm}$ ) lies in the  $ab$  plane,<sup>3</sup> however, the electrical conductivity is also very high in this plane.<sup>4,5</sup>

Such an anisotropy is also reflected in the grain growth habit. Typical microstructure of BIT-based ceramics shows big platelet-like grains growing

preferentially in the  $ab$  plane. As it has been shown,<sup>6</sup> the aspect ratio of the platelets plays a critical role on the conductivity of BIT ceramics. Therefore, in order to obtain an useful piezoelectric from these ceramics, electrical conductivity must be decreased. It is also well known that donor doping decreases conductivity<sup>6,7</sup> and that processing can drastically modify the electrical behaviour of  $\text{Bi}_4\text{Ti}_3\text{O}_{12}$  by changing the platelets growth habit.<sup>8</sup> W-doping has been reported to decrease electrical conductivity<sup>6,8,9</sup> but at present relatively high piezoelectric properties of W-doped BIT have not been reported. The objective of this work is to study the effect of the addition of different amounts of  $\text{WO}_3$  as donor dopant on the sintering, microstructure and electrical properties of BIT based ceramics to improve its piezoelectric behaviour.

## 2. Experimental procedure

$\text{Bi}_4\text{Ti}_{2.95}\text{W}_x\text{O}_{11.9+3x}$  (with  $0.02 < x < 0.15$ ) ceramics were prepared by a chemical route, using the hydroxide coprecipitation method. Titanium tetrabutoxide  $\text{Ti}(\text{C}_4\text{H}_9\text{O})_4 \cdot \text{C}_4\text{H}_9\text{OH}$  (Alfa Aesar),  $\text{Bi}(\text{NO}_3)_3 \cdot 5\text{H}_2\text{O}$  (Riedel) and  $\text{W}(\text{C}_2\text{H}_5\text{O})_6$  (Alfa Aesar) were used as  $\text{TiO}_2$ ,  $\text{Bi}_2\text{O}_3$  and  $\text{WO}_3$  precursors, respectively. Stoichiometric amounts of  $\text{Ti}^{4+}$  and  $\text{Bi}^{3+}$  precursors were

\* Corresponding author. Tel.: +91-735-5840; fax: +735-5843.

E-mail address: [mvillegas@icv.csic.es](mailto:mvillegas@icv.csic.es) (M. Villegas).

dissolved in ethanol,  $\text{NH}_4\text{OH}$  was then added to this solution up to  $\text{pH}=9$ , to achieve the complete coprecipitation of  $\text{Bi}(\text{OH})_3$  and  $\text{Ti}(\text{OH})_4$ . The coprecipitated powders were washed and redispersed up to  $\text{pH}=7$ . After drying an amorphous powder was obtained. The coprecipitated powders were air-calcined at  $650^\circ\text{C}$  for 1 h and attrition milled for 2 h in ethanol. After drying and sieving, the calcined powders were redispersed in ethanol and the corresponding amount of  $\text{WO}_3$  precursor was added to these suspensions. The BIT doped powders were dried again, granulated and uniaxially pressed. For comparison, pure  $\text{Bi}_4\text{Ti}_3\text{O}_{12}$  was prepared and dispersed in the same way. The BIT based materials were sintered in air between  $950$  and  $1150^\circ\text{C}$  (soaking time, 2 h). Compositions will be referred as follows: BIT, BITW2 ( $x=0.02$ ), BITW5 ( $x=0.05$ ), BITW8 ( $x=0.08$ ) and BITW15 ( $x=0.15$ ).

The apparent density of the sintered samples was measured by the Archimedes method in water and the weight losses were determined by weight. Sintered samples were characterized by XRD diffraction and the lattice parameters were determined in powder samples using Si as internal standard. The microstructure of the sintered compacts was studied by Scanning Electron Microscopy (Carl Zeiss DSM 950) on polished and thermally etched surfaces. The grain size of the platelets was determined using an image analyzer (Leica Q-win). Electrical measurements were carried out on Ag-electroded disks. Dielectric characterization was performed using a HP4192A impedance analyzer in the temperature range  $25$ – $740^\circ\text{C}$ . Selected samples were poled at  $180^\circ\text{C}$  during 1 h applying a dc field of  $60\text{ kV/cm}$ .

### 3. Results

#### 3.1. Sintering

Fig. 1 shows the densification curves for  $\text{Bi}_4\text{Ti}_3\text{O}_{12}$  and  $\text{Bi}_4\text{Ti}_{2.95}\text{W}_x\text{O}_{11.9+3x}$  ceramics. As it can be seen, the maximum density in BITW2 ceramics was obtained at  $1000^\circ\text{C}$ , whereas in the case of BITW15 the higher densification was produced at  $1100^\circ\text{C}$ . The other ceramics, BIT, BITW5 and BITW8 reached the maximum density at  $1050^\circ\text{C}$ . Weight losses were very low in all cases and, as expected, grew with temperature, being very similar in the case of BIT, BITW5 and BITW8 (up to  $1050^\circ\text{C}$  in the latter) and somewhat higher for BITW2 and BITW15.

#### 3.2. Structural characterization

Fig. 2 shows the XRD patterns of BIT based materials at two different temperatures. At low temperature no secondary phases are observed in any material.

However, at high temperatures secondary phases of the type  $\text{Bi}_2\text{Ti}_4\text{O}_{11}$  and  $\text{Bi}_6\text{Ti}_3\text{WO}_{18}$  are present, specially in BITW15 ceramics.

In Fig. 3 the variation of the  $c$  lattice parameter for the different ceramics is shown for samples at maximum density. As it can be seen, when samples have reached the maximum density ( $1050^\circ\text{C}$  for BIT, BITW2 and BITW5,  $1000^\circ\text{C}$  for BITW2 and  $1100^\circ\text{C}$  for BITW15) the  $c$  lattice parameter remained unchanged for BIT and BITW2 and then it decreases as  $\text{WO}_3$  content increases.

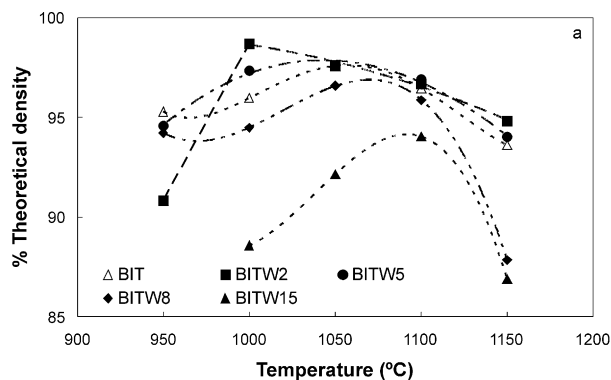


Fig. 1. Densification curves as a function of temperature for  $\text{Bi}_4\text{Ti}_3\text{O}_{12}$  and  $\text{Bi}_4\text{Ti}_{2.95}\text{W}_x\text{O}_{11.9+3x}$  ceramics. (Soaking time = 2 h).

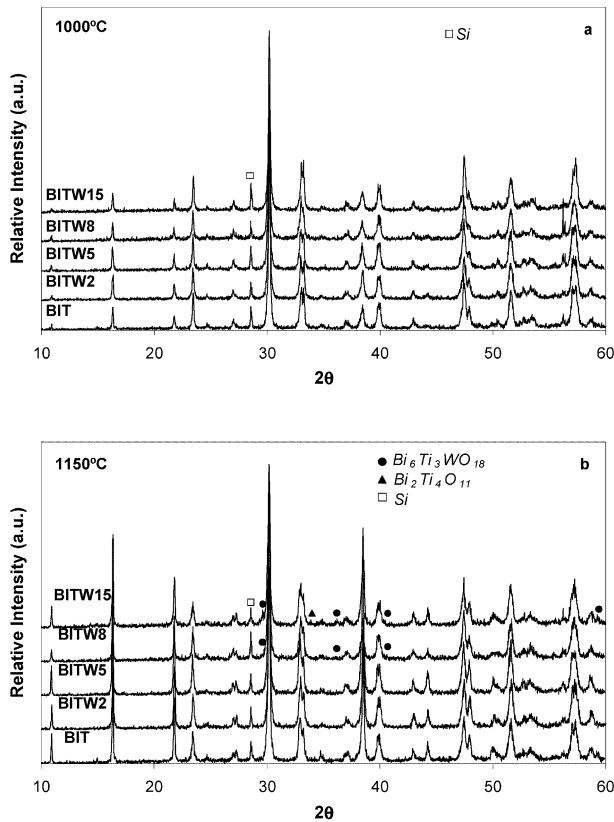


Fig. 2. XRD Patterns of  $\text{Bi}_4\text{Ti}_3\text{O}_{12}$  and  $\text{Bi}_4\text{Ti}_{2.95}\text{W}_x\text{O}_{11.9+3x}$  sintered samples. (a)  $1000^\circ\text{C}$  and (b)  $1150^\circ\text{C}$  (soaking time = 2 h).

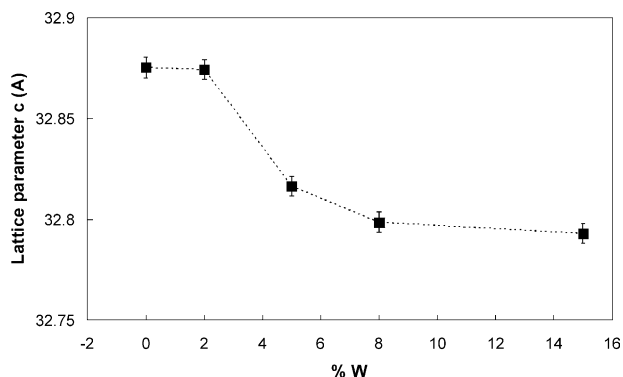


Fig. 3. Variation of lattice parameter  $c$  for samples at maximum density.

For  $x > 0.08$  the  $c$  lattice parameter remains almost constant.

### 3.3. Microstructure evolution

Fig. 4 shows the SEM micrographs of the sintered BIT-based ceramics at the temperature corresponding to the maximum density. As it can be seen, the addition of  $\text{WO}_3$  decreased platelet size and, in general, as the dopant concentration increases more homogeneous grain size is observed, specially for  $x \geq 0.08$ .

### 3.4. Electrical properties

Dielectric constant and dielectric losses as a function of temperature at 1MHz are shown in Fig. 5. Dielectric constant increases with  $\text{WO}_3$  amount up to  $x = 0.08$ . The curve corresponding to pure BIT ceramics showed a different shape at low temperatures ( $T > 400$  °C). A very important effect is observed in dielectric losses (Fig. 5b). The addition of  $\text{WO}_3$  drastically decreased them, especially when  $x \geq 0.08$  and remained in very low up to very high temperatures ( $\approx 650$  °C).

Fig. 6 shows the Arrhenius plots of the electrical conductivity for the different BIT based ceramics. As expected, bulk electrical conductivity decreased with the amount of donor dopant. BITW2 and BITW5 presented very similar conductivity, with a reduction of about one order of magnitude and a similar activation energy when compared with pure BIT. On the contrary, the activation energy of BITW8 and BITW15 is different than in the other ceramics and the decrease in conductivity is about two orders of magnitude in both materials, which presented a very similar behavior.

BITW8 and BITW15 ceramics were poled and Table 1 resume the piezoelectric properties.

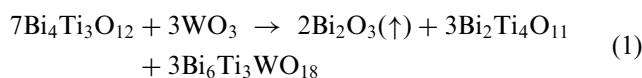
## 4. Discussion

Densification behavior of undoped BIT, BITW5 and BITW8 is quite similar, reaching maximum density at

Table 1  
Piezoelectric properties of BITW8 and BIT15 ceramics

	$T$ (°C)	$K_3^T$	$\tan \delta$ (%)	$d_{33}$ (pC/N)
$\text{Bi}_4\text{Ti}_{2.95}\text{W}_{0.08}\text{O}_{12.14}$	1050	179	1.42	19
	1100	170	1.53	15
$\text{Bi}_4\text{Ti}_{2.95}\text{W}_{0.15}\text{O}_{12.35}$	1050	185	0.76	20
	1100	179	1.21	16

the same temperature and showing low weight losses up to maximum density. This seems to indicate that the role played by  $\text{WO}_3$  is to control the kinetics of the grain growth mechanism, being incorporated to the BIT lattice at the last sintering stage. For the samples BITW8 and BITW15, the stoichiometry of this Aurivillius type compounds is exceeded. In this manner, secondary phases appeared related also to a strong increase of the weight losses at temperatures above the maximum densification. According to the XRD data, the following reaction can be proposed:



Lattice parameters dependence on the  $\text{WO}_3$  concentration (Fig. 3) is in agreement with the incorporation of  $\text{WO}_3$  into the BIT lattice for samples showing the maximum density.

For the BITW2 ceramics densification occurs at lower temperatures even if compared to undoped BIT. Because of the stoichiometry, BITW2 is strongly oxygen deficient and this seems to improve the diffusion mechanisms that lead to densification. Grain size in BITW2 is lower than for undoped BIT which indicates that  $\text{WO}_3$  is controlling grain growth in spite of the high oxygen deficiency.

For BITW15 the variation of  $c$  lattice parameter points out that not all the  $\text{WO}_3$  is incorporated into the BIT lattice. However, in the samples with maximum density the presence of secondary phases has been not detected by XRD, but they can exist in a small amount, below the detection limit of the technique. The excess of  $\text{WO}_3$ , which is highly refractory, seems to delay the diffusion mechanisms that leads to densification. This can be due to two effects, one the reduction of the oxygen vacancies, that plays an important role in densification or, second, the coalescence of  $\text{WO}_3$  particles in excess which would exert a pinning effect inhibiting densification. As occurred with the other BIT based ceramics, higher the amount of  $\text{WO}_3$  lower the diffusion kinetics that lead to grain growth, with the platelets size being smaller.

Electrical properties were modified by the amount of dopant, and dielectric constant increased with  $\text{WO}_3$  concentration up to  $x = 0.08$ . In BIT ceramics, the

different shape of the dielectric constant vs temperature, the high dielectric constant and dielectric losses are due to the accumulation of spatial charges.<sup>10</sup> It is important to point out that the addition of  $\text{WO}_3$  drastically reduced dielectric losses as consequence of the reduction of electrical conductivity (see Fig. 6) due to donor doping and that they began to increase at very high temperature ( $T > 650\text{ }^\circ\text{C}$ ) for  $x \geq 0.08$ , which allowed the polarization of those ceramics.

As expected, the electrical conductivity in BITW2 and BITW5 decreased one order of magnitude when

compared with BIT. The slope of the Arrhenius plots of BITW2 and BITW5 ceramics is very similar indicating that the conduction mechanisms is the same and only a reduction of charge carriers is produced when doping with  $\text{WO}_3$  up to  $x = 0.05$  (see Fig. 6). On the contrary, when  $x \geq 0.08$ , a more pronounced decrease in the electrical conductivity is produced along with a change in the slope of the Arrhenius curves which indicates that a different mechanism with different activation energy might be controlling the electrical conductivity in BITW8 and BITW15 ceramics. The presence of

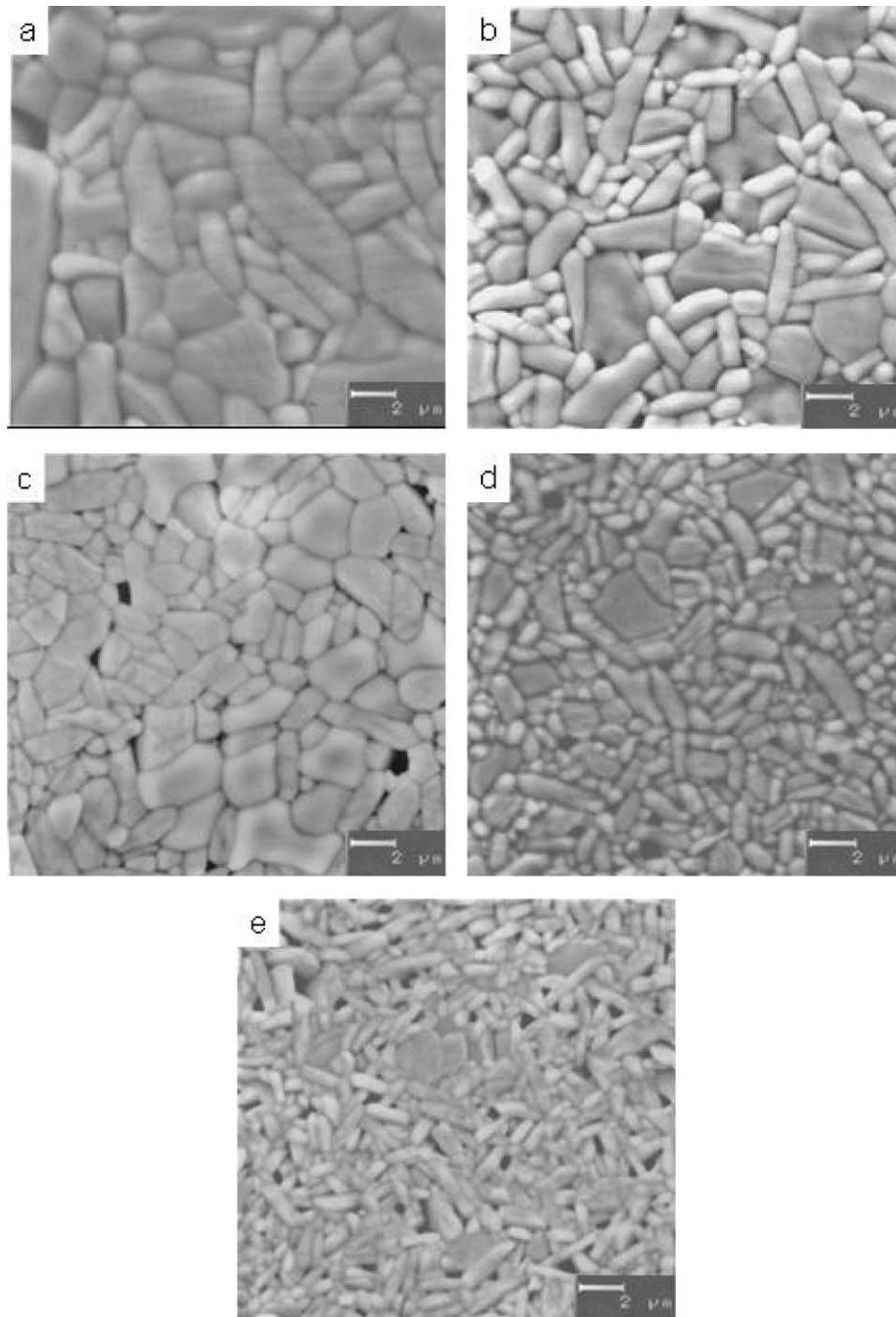


Fig. 4. SEM micrographs of polished and thermally etched surfaces of (a) BIT, (b) BITW2, (c) BITW5, (d) BITW8 and (e) BITW15.

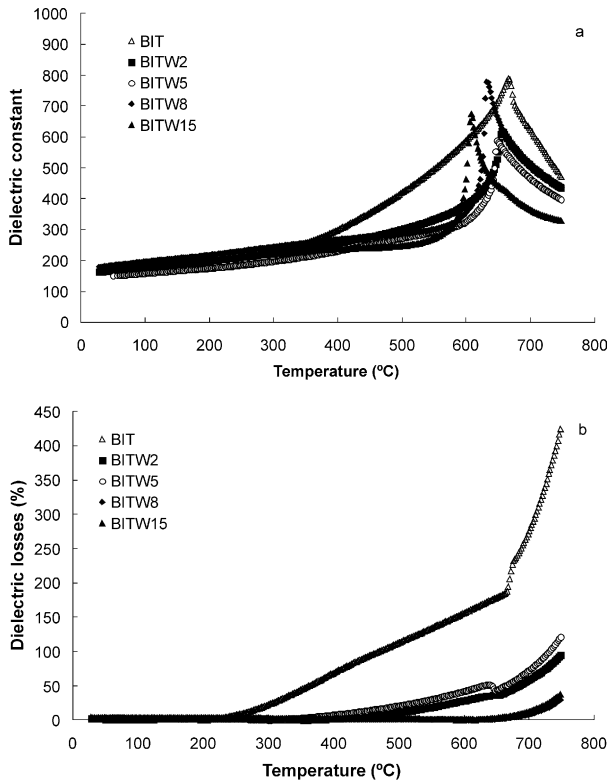


Fig. 5. (a) Dielectric constant and (b) dielectric losses as a function of temperature for BIT-based ceramics (samples at maximum density).

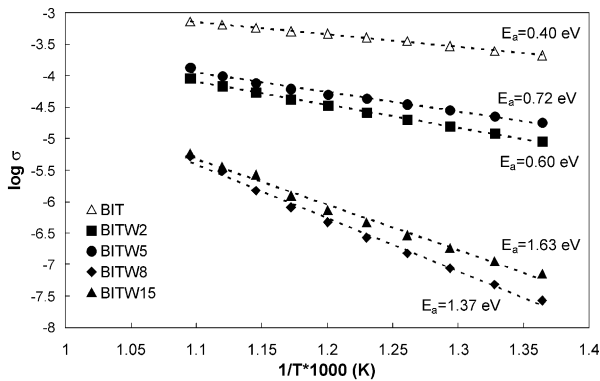


Fig. 6. Arrhenius plots of the electrical conductivity for BIT-based ceramics (samples at maximum density).

secondary phase or segregated phases at grain boundaries which impede the percolation of the ab planes of the platelets may decrease electrical conductivity in those materials.

The decrease in the conductivity in donor doped BIT ( $x \geq 0.08$ ) allowed ceramics to be poled at high temperatures (180 °C) and with high electric fields (60 kV/cm) which resulted in a relatively large longitudinal piezoelectric constant ( $d_{33} \sim 20$  pC/N).

## 5. Conclusions

Densification mechanisms of bismuth titanate based ceramics doped with  $\text{WO}_3$ ,  $\text{Bi}_4\text{Ti}_{2.95}\text{W}_x\text{O}_{11.9+3x}$ , are controlled by oxygen vacancy concentration which improve the diffusion mechanisms that lead to densification. When secondary phases appeared, as consequence of a no-complete incorporation of  $\text{WO}_3$  into the BIT lattice, a pinning effect which inhibits densification and control grain growth can be also present. Electrical properties depended, as expected, on the amount of dopant, and also on the presence of secondary phases which modified electrical conductivity mechanism, reducing both dielectric losses and electrical conductivity allowing the polarization of the ceramics with a high level of dopant ( $x \geq 0.08$ ) which resulted in relatively high piezoelectric constants  $d_{33} = 20$  pC/N.

## Acknowledgements

This research was supported by the Spanish Comisión Interministerial de Ciencia y Tecnología (CICYT) under Project MAT2001-1682-C02-01.

## References

1. Aurivillius, B., Mixed bismuth oxides with layer lattices. *Ark. Kemi*, 1949, **1**, 463–480.
2. Dorrian, J. F., Newnham, R. E. and Smith, D. K., Crystal structure of  $\text{Bi}_4\text{Ti}_3\text{O}_{12}$ . *Ferroelectrics*, 1971, **3**, 17–21.
3. Cummings, S. E. and Cross, L. E., Electrical and optical properties of ferroelectric  $\text{Bi}_4\text{Ti}_3\text{O}_{12}$  single crystals. *J. Appl. Phys.*, 1968, **39**, 2268–2274.
4. Fouskova, A. and Cross, L. E., Dielectric properties of bismuth titanate. *J. Appl. Phys.*, 1970, **41**, 2834–2838.
5. Takenaka, T. and Sakata, K., Grain orientation effects and electrical properties of bismuth layer structured ferroelectric  $\text{Pb}_{1-x}(\text{Na/Ce})_x\text{Bi}_4\text{Ti}_4\text{O}_{15}$  solid solution. *J. Appl. Phys.*, 1984, **55**, 1092.
6. Villegas, M., Caballero, A. C., Moure, C., Durán, P. and Fernández, J. F., Factors affecting the electrical conductivity of donor-doped  $\text{Bi}_4\text{Ti}_3\text{O}_{12}$  piezoelectric ceramics. *J. Am. Ceram. Soc.*, 1999, **82**, 2411–2416.
7. Shulman, H. S., Testorf, M., Damjanovic, D. and Setter, N., Microstructure, electrical conductivity and piezoelectric properties of bismuth titanate. *J. Am. Ceram. Soc.*, 1996, **79**, 3124–3128.
8. Villegas, M., Caballero, A. C. and Fernández, J. F., Modulation of electrical conductivity through microstructural control in  $\text{Bi}_4\text{Ti}_3\text{O}_{12}$ -based piezoelectric ceramics. *Ferroelectrics*, 2002, **267**, 165–173.
9. Lopatin, S. S., Lupeiko, T. G., Vasiltsova, T. L., Basenki, N. I. and Berlizev, I. M., Properties of bismuth titanate ceramic modified with group V and VI elements. *Inorg. Mater.*, 1988, **24**, 1328–1331.
10. Ehara, S., Muramatsu, K., Shimazu, M., Tanaka, J., Tsukioka, M., Mori, Y., Hattori, T. and Tamura, H., Dielectric properties of  $\text{Bi}_4\text{Ti}_3\text{O}_{12}$  below the Curie temperature. *Jpn. J. Appl. Phys.*, 1981, **20**, 877–881.